21-cm intensity mapping interferometers: a new window on large-scale structure

Martin White (UCB/LBNL)

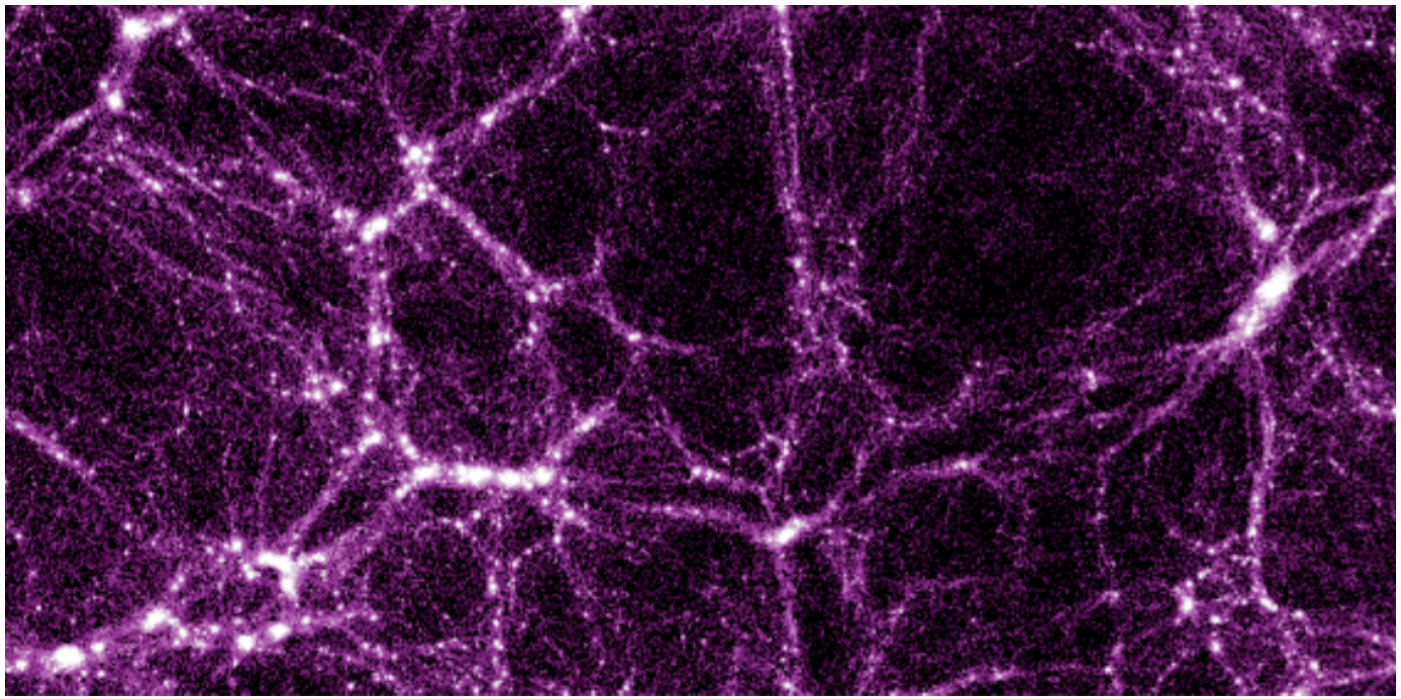

http://mwhite.berkeley.edu/Talks

Outline

Large-scale structure is one of our premier laboratories for fundamental physics, cosmology and astrophysics. Traditionally it has been done with galaxy redshift surveys, working outwards from $z \simeq 0$. But there may be other ways ...

- Cosmic brunch.
- Reminder of 21 cm physics.
- Interferometer basics.
- HI at "intermediate" redshift.
- Intensity mapping, foregrounds & wedges
- Modeling HI observations.
- Resources

Cosmic brunch ($2 < z < 6$)

- There is $3\times$ more volume at $2 < z < 6$ than $z < 2$.
- Less evolved, better understood, more correlated with $\delta_{\rm init}$.
- All standard mode-counting constraints improve by $5\times$:
  - $P(k)$ shape, BAO, m_ν, $dn/d\ln k$, $N_{\rm eff}$, etc.
  - Features, higher-order correlators, ...

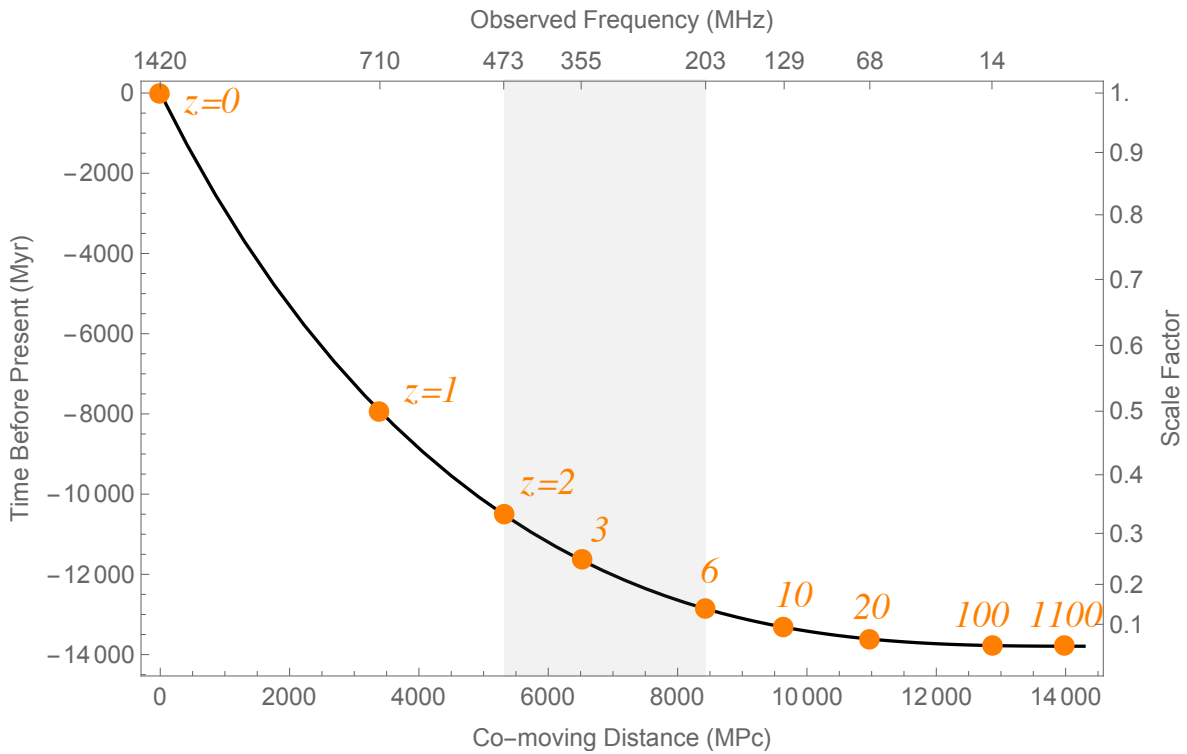

arXiv:1810.09572

Volume and modes

Note: $z = 6$ is over half way to the edge of the Universe!

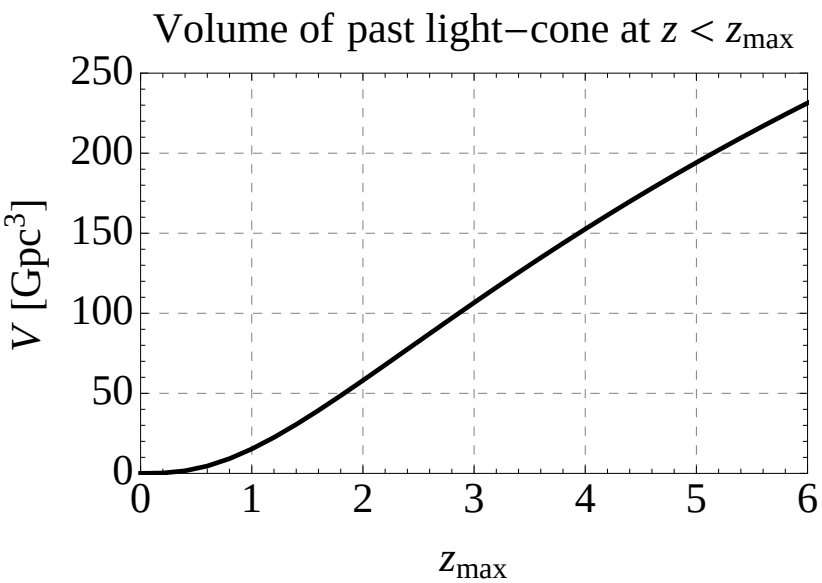

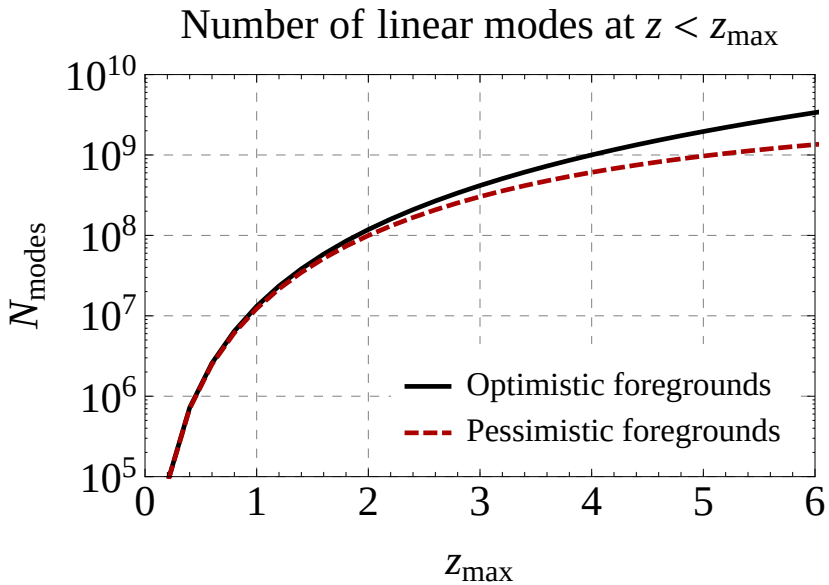

arXiv:1810.09572

BAO

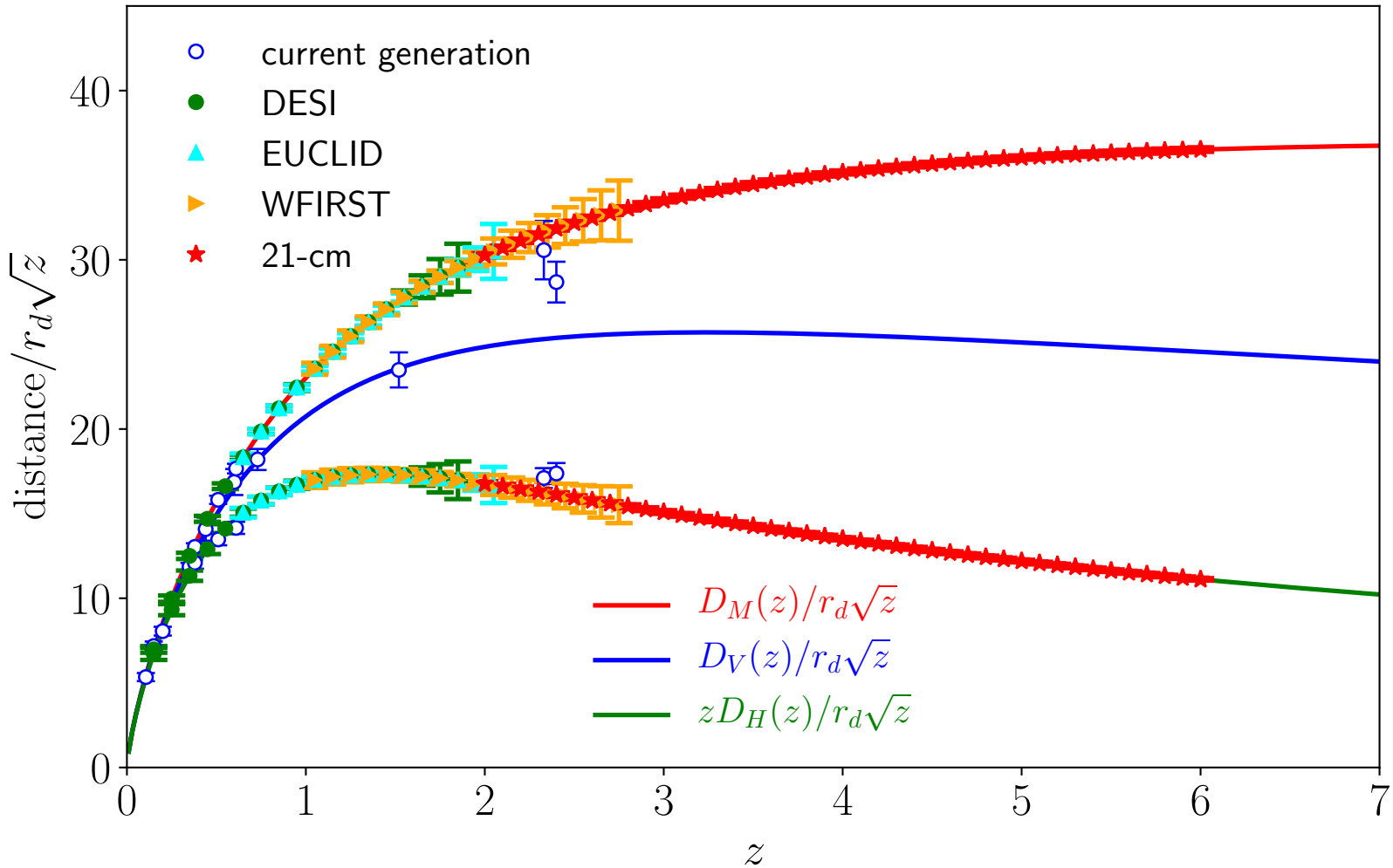
current generation
DESI
EUCLID
WFIRST
21-cm
$D_M(z)/r_d\sqrt{z}$
$D_V(z)/r_d\sqrt{z}$
$zD_H(z)/r_d\sqrt{z}$
distance/$r_d\sqrt{z}$
z
0
10
20
30
40
0
1
2
3
4
5
6
7

Growth rate

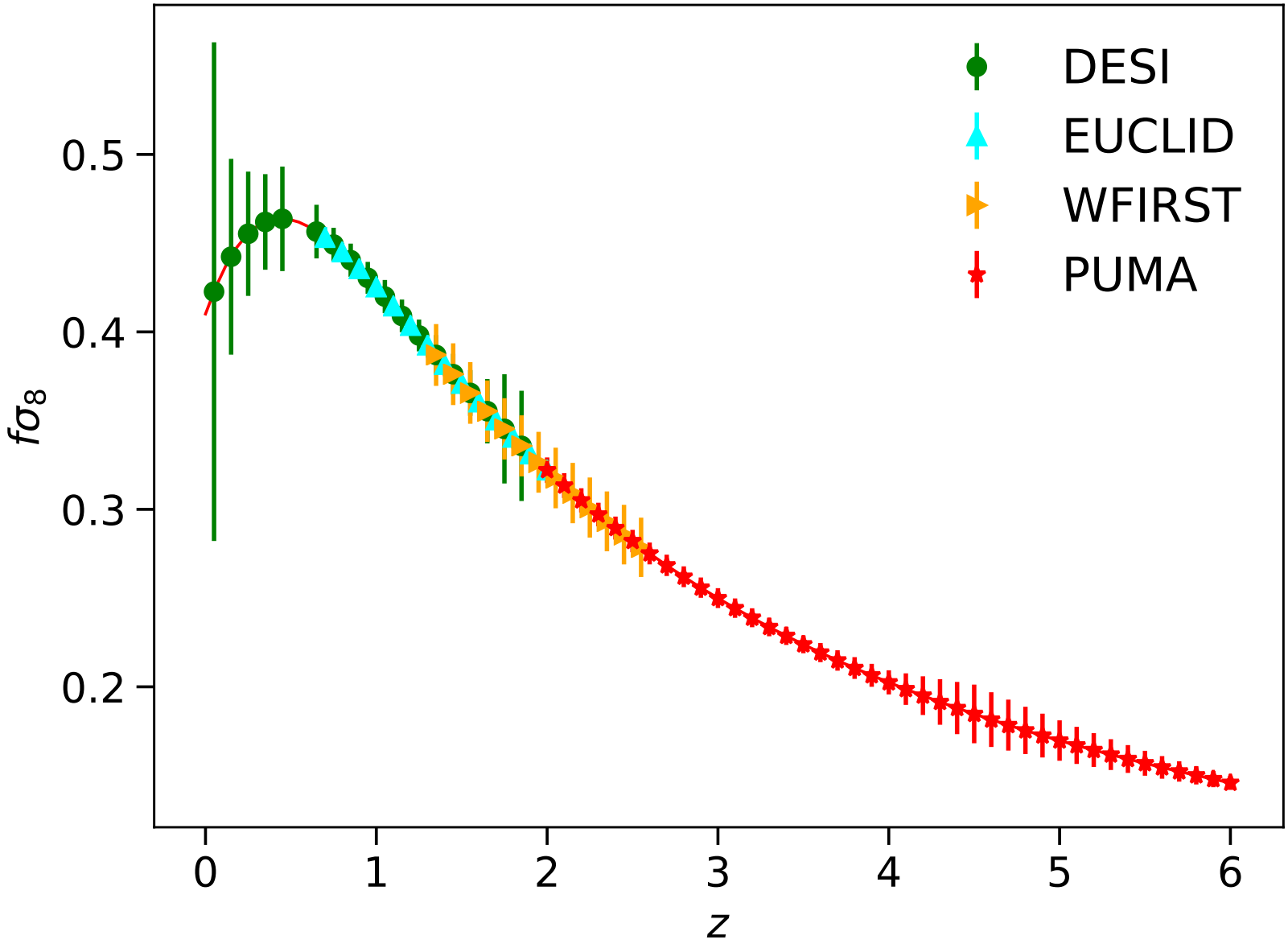

... and other things

- Search for voids and protoclusters [arxiv:1705.09669]
- Weak lensing and linear field reconstruction.
- Calibrating dN/dz for photo-z samples.
- Secondary CMB anisotropies.
- Multi-messenger and time-domain science.

Basics of 21 cm

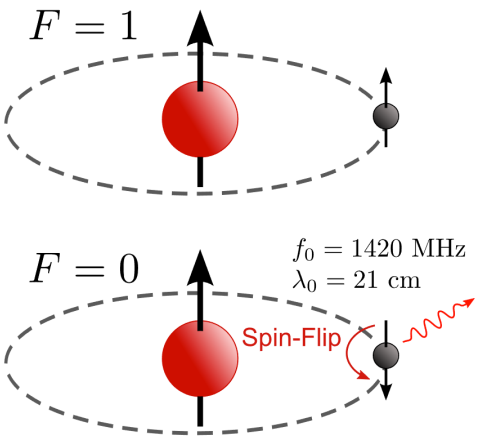

(Wikipedia)

- Hyperfine (mag. dip.) transition of HI
- Spin-spin coupling between $p + e$

$$\begin{aligned} \Delta E &= 4 g_p \hbar^4 / (3 m_p m_e^2 c^2 a^4) \\ &\simeq 6\,\mu\,\mathrm{eV} \end{aligned}$$

- Very rare transition per atom ($\propto \omega^3 \mu^2$):

$$\begin{aligned} A_{10} &= \frac{64\,\pi^4\,\mu_B^2}{3\,h\,\lambda^3} \\ &\simeq 2.85 \times 10^{-15}\,\mathrm{s}^{-1} \end{aligned}$$

- Little absorption or confusion (no line at 710 MHz!), but long wavelength.

Aside: The semi-relativistic Hamiltonian

$$H_D \approx \underbrace{\frac{\mathbf{p}^2}{2m} + V}_{\text{Schrodinger}} \underbrace{- \overbrace{\frac{\mathbf{p}^4}{8m^3}}^{\text{SR}} - \overbrace{\frac{\hbar^2}{4m^2}\frac{\partial V}{\partial r}\frac{\partial}{\partial r}}^{\text{Darwin}} + \overbrace{\frac{1}{2m^2 r}\frac{\partial V}{\partial r}\mathbf{S}\cdot\mathbf{L}}^{\text{spin-orbit}}}_{\text{fs}\sim\mathcal{O}(v^2)}$$

$$\underbrace{+\frac{q}{2m}\left[\mathbf{p}\cdot\mathbf{A} + \mathbf{A}\cdot\mathbf{p}\right] - 2\frac{\mu_B}{\hbar}\overbrace{\mathbf{S}\cdot\mathbf{B}}^{\text{mag.dip.}}}_{\text{hf}\sim\mathcal{O}([m_e/m_p]v^2)} + \underbrace{\frac{q^2}{2m}\mathbf{A}\cdot\mathbf{A}}_{\text{2-photon}}$$

Brightness temperature

Rather than intensity we talk about measuring fluctuations in brightness temperature [$I_\nu = 2k_B T_B(\nu/c)^2$] around the mean: $\bar{T}$. The mean cosmological brightness temperature for 21-cm is

$$\begin{aligned} \bar{T} &= \frac{3h_P c^3 A_{10}}{32\pi\, m_H k_B \nu_{21}^2} \frac{(1+z)^2}{H(z)}\, \rho_{HI} \\ &\simeq 188h\,(1+z)^2 E(z)\Omega_{HI}(z)\,\mathrm{mK} \end{aligned}$$

Note that unlike galaxy surveys we don't know $\bar{T}$ because we don't really know Ω_{HI} all that well [1506.02037]:

$$\Omega_{HI}(z) = (4\pm?)\times 10^{-4}(1+z)^{0.6}\, E^{-2}(z)$$

This means the amplitude of the fluctuations (bias) is degenerate with $\bar{T}$.

Big radio telescopes

- Long wavelength $\Rightarrow$ low resolution for single dish.
- Very weak (record holder: $z = 0.376$ from 178hr on VLA)
- Need big arrays for sensitivity (+ resolution)
- Many elements and channels $\Rightarrow$ big data problem!
- Radio arrays have not been big enough for high z surveys ...
- ... because we haven't been able to handle the data!

The steady advance of computing and signal processing capability paid for by the telecommunications industry and chip manufacturers is making this tractable!

Broadband receivers make large z range possible in a single instrument.

Promise: the web at $z = 3$

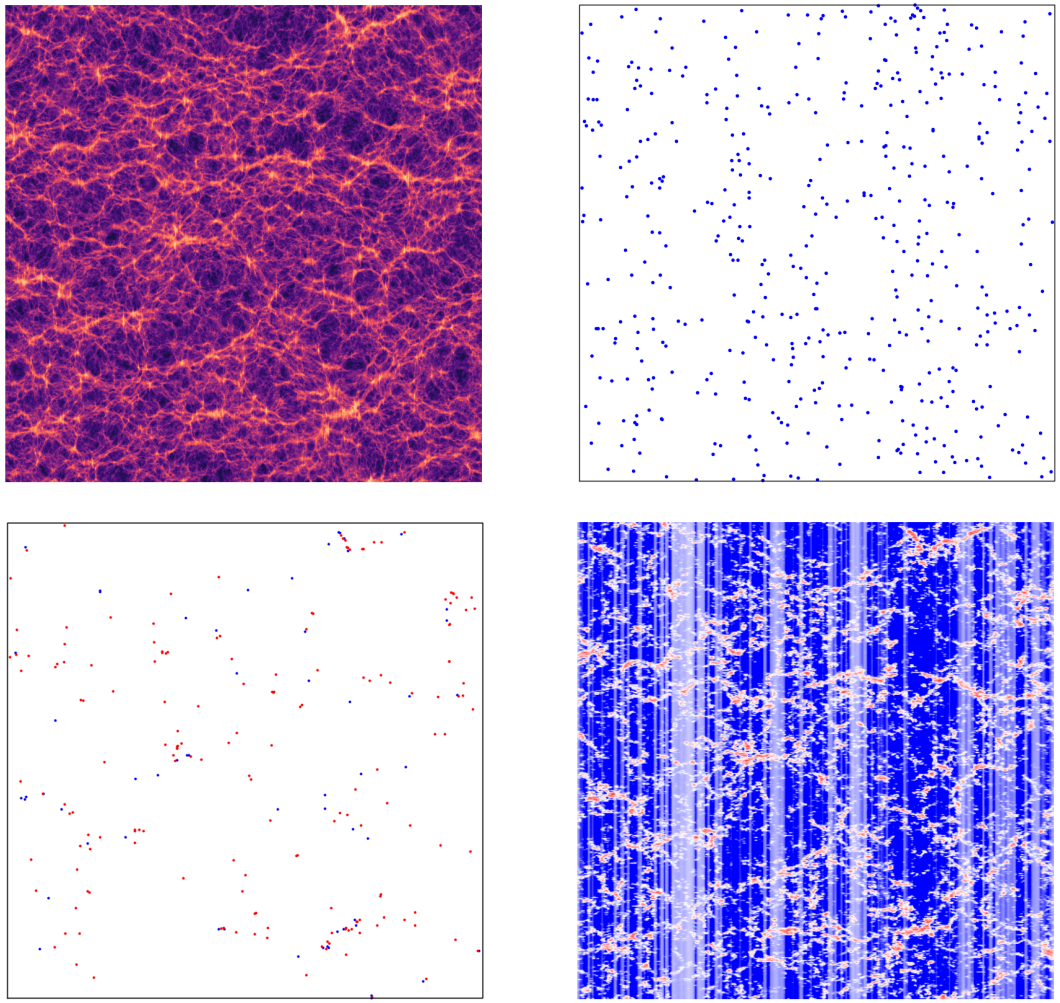

arXiv:1810.09572

Interferometer basics: Visibilities

In an interferometer the fundamental data is the correlation between two feeds (or antennae), known as a visibility.

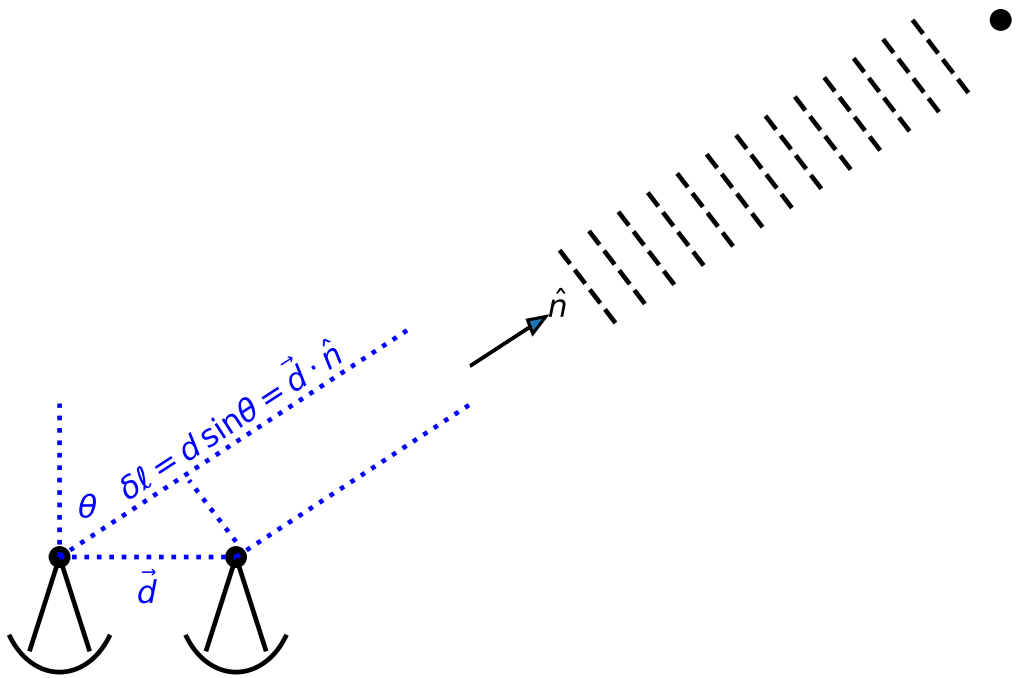

$$V_{ij} = \left\langle E_i E_j^{\star} \right\rangle_{\text{time}}$$

Interferometer basics: Visibilities

In an interferometer the fundamental data is the correlation between two feeds (or antennae), known as a visibility. For an intensity measurement the visibility is

$$V_{ij} \propto \int d^2\hat{n}\; A^2(\hat{n}) T(\hat{n})\; e^{2\pi i \hat{n}\cdot\vec{u}_{ij}}$$

where

- $T(\hat{n})$ is the brightness temperature in the sky direction $\hat{n}$,
- A is the primary beam (assumed the same for all feeds) and
- $\vec{u}_{ij}$ is the difference in position vectors of the i^{th} and j^{th} feeds in units of the observing wavelength.

An interferometer works natively in (angular) Fourier space. The $\vec{\ell}$-modes measured are set by the spacing of the feeds.

Beams and window functions

- The feed "illuminates" the dish to form a beam on the sky.
- Fraunhöfer diffraction is essentially just FTs:

$$A(\hat{n}) \sim \left| \mathrm{FT}\left[\vec{E}\right] \right|^2$$

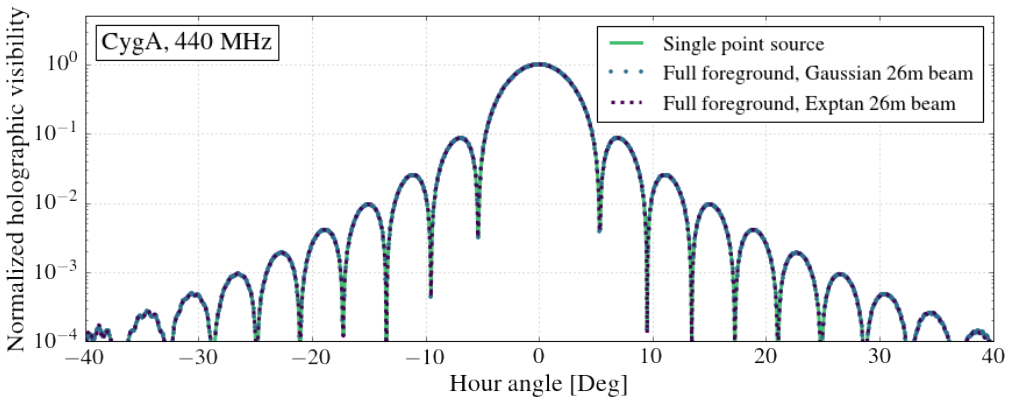

(Berger++16)

- However we want the FT of the beam!
- This is just the auto-correlation of the $\vec{E}$-field response of the telescope – defines the window function in $\vec{u}$ space.
- Really measure FT of sky convolved with this window.

Interferometer basics: Visibilities

Each visibility measures the FT of the sky, "averaged" over a small region of $\vec{\ell}$-space. The $\vec{\ell}$ mode is determined by the dish spacing while the averaging region is determined by the dish diameter.

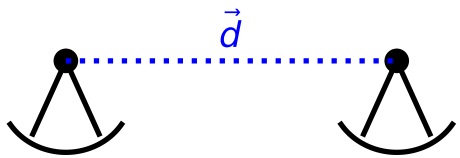

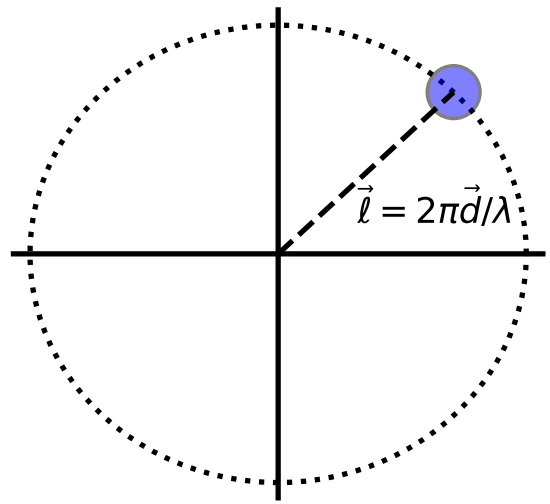

As the sky rotates over the fixed dishes, the visibility sweeps a circle in the $\vec{\ell}$-plane of fixed $|\vec{\ell}|$.

Measuring a power spectrum

There are numerous ways one can estimate a power spectrum from the visibility data, some are discussed in these recent papers:

- Morales+04
- Parsons+12
- Shaw+14, 15
- Pober+16
- Zheng+17
- Morales+19

and the many references therein.

The *m*-mode formalism and transiting telescopes

How to analyze data from transiting telescopes?

Focus today on "*m*-mode formalism" ...

Shaw+14, 15

The *m*-mode formalism and transiting telescopes

It is anticipated that data from transiting telescopes will be analyzed differently than for traditional, dish-based, tracking interferometers. If the beam transfer function at azimuth ϕ is

$$B_{ij}(\hat{n};\phi) \propto A^2(\hat{n};\phi)\,\exp\left[2\pi i\,\hat{n}\cdot\vec{u}_{ij}(\phi)\right]$$

then

$$V_{ij}(\phi) = \int d^2\hat{n}\; T(\hat{n}) B_{ij}(\hat{n};\phi)$$

(plus noise, of course). Defining

$$V_{ij}^m = \int \frac{d\phi}{2\pi} e^{-im\phi} V_{ij}(\phi)$$

The m-mode formalism and transiting telescopes

Expanding T and $B_{ij}(\phi)$ into spherical harmonics

$$\begin{aligned} T(\hat{n}) &= \sum_{\ell m} a_{\ell m}\, Y_{\ell m}(\hat{n}) \\ B_{ij}(\hat{n};\phi) &= \sum_{\ell m} B^{ij}_{\ell m}\, Y^{\star}_{\ell m}(\hat{n}) \end{aligned}$$

the V^m_{ij} just give $B^{\ell m}_{ij}$ at $\phi = 0$ (i.e. the rotation by ϕ is undone by the $\exp[-im\phi]$ in the V_m definition) so

$$V^m_{ij} = \sum_{\ell} B^{\ell m}_{ij} a_{\ell m}$$

Multi-frequency angular power spectrum (MAPS)

So now when we square up V_{ij}^{m} we get powers of $B_{ij}^{\ell m}$ times $\langle a^{\star}_{\ell m} a_{\ell' m'} \rangle = C_{\ell} \delta_{\ell \ell'} \delta_{m m'}$.
The C_{ℓ} evaluated between two frequency (redshift) shells is a complete summary of the 2-point information as is known as the multifrequency angular power spectrum (MAPS).
For sufficiently large ℓ we can relate it to the usual 3D power spectrum as:

$$
\begin{aligned}
C_{\ell}(\nu_1, \nu_2) &= C_{\ell}(\Delta\nu; \bar{\nu}) \\
&\simeq C_{\ell}(s_{\parallel}; d) \\
&\simeq \int_{-\infty}^{\infty} \frac{dk_{\parallel}}{2\pi\, d^2}\; P(\ell = k_{\perp} d, k_{\parallel}) e^{i k_{\parallel} s_{\parallel}} \\
&= \int_{0}^{\infty} \frac{dk_{\parallel}}{\pi\, d^2}\; P(\ell = k_{\perp} d, k_{\parallel}) \cos\left(k_{\parallel} s_{\parallel}\right)
\end{aligned}
$$

Aside: flat-sky derivation

Consider the correlation of two points separated by angle $\theta = s_\perp/d$ and radial distance $s_\parallel$:

$$
\begin{aligned}
w(\theta) &= \int \frac{d^3k}{(2\pi)^3} P\left(\left|\vec{k}_\perp\right|, k_\parallel\right) e^{i\vec{k}\cdot\vec{s}} \quad (\text{fixed } s_\perp, s_\parallel) \\
&= \int \frac{k_\perp\, dk_\perp}{2\pi} \int \frac{dk_\parallel}{2\pi} P(k_\perp, k_\parallel) J_0(k_\perp d\theta) e^{ik_\parallel s_\parallel} \\
&\simeq \sum_\ell \frac{2\ell+1}{4\pi} P_\ell(\cos\theta) \left(\int \frac{dk_\parallel}{2\pi\, d^2} P(k_\perp, k_\parallel) e^{ik_\parallel s_\parallel} \right)
\end{aligned}
$$

where in the 2^{nd} line I have used the Rayleigh expansion of the plane wave and in the last line I have used $J_0(\ell\theta) \approx P_\ell(\cos\theta)$ for $\theta \ll 1$ and $\ell = k_\perp d \gg 1$.
The angular power spectrum is then the term in parentheses.

For non-flat-sky limit see arxiv:1803.08185.

Visibilities to Bandpowers

Let us consider a transit interferometer, with data being analyzed in the m-mode formalism.
For baselines (pairs of receivers) $I = (ab)$ and $J = (cd)$ the visibility two-point function is

$$\langle V_I^m(\nu_1) V_J^{n\star}(\nu_2) \rangle = \delta_{mn} \sum_\ell B_I^{\ell m} B_J^{\ell m\star} C_\ell(\nu_1, \nu_2)$$

and we will be given $B_J^{\ell m}$.

For antennae on the equator looking directly overhead an EW baseline has $B_J^{\ell m}$ peaked around $\ell \sim m \sim 2\pi(d/\lambda)$ while a NS baseline has $B_J^{\ell m}$ peaked around $\ell \sim 2\pi(d/\lambda)$ and $m = 0$.

Visibilities to Bandpowers

Define $\mathcal{V}_B = \sum_{IJm} \langle V_I^m V_J^{m\star} \rangle$ for I and J in baseline distance bin B, then

$$\begin{aligned}
\mathcal{V}_B &= \sum_{IJ} \sum_{\ell m} B_I^{\ell m} B_J^{\ell m \star} \; C_\ell(\nu_1, \nu_2) \\
&\equiv \sum_{\ell} \mathcal{B}_{B\ell} \; C_\ell(\nu_1, \nu_2) \\
&= \sum_{L} \left(\sum_{\ell} \mathcal{B}_{B\ell} \Pi_{\ell L} \right) C_L(\nu_1, \nu_2) = \sum_{L} \mathcal{B}_{BL} C_L(\nu_1, \nu_2)
\end{aligned}$$

where in the last step we introduced a "projection" or "indicator" operator $\Pi_{\ell L}$ which is one when ℓ is in bin L else zero and we assumed C_ℓ is a constant within that bin (or we're estimating some average value).
Can fit model or use GLS.

Modeling 21 cm

- In the "intermediate" redshift Universe ($0.5 < z < 5$) most of the Hydrogen is ionized.
- HI signal comes from self-shielded regions
  - Most likely at densities between the outskirts of disks and where the gas becomes molecular.
- Hard problem computationally.
- Few constraints observationally:
  - Galaxy surveys at $z < 0.1$ (mass functions).
  - DLA abundance observations (for Ω_{HI}) at $z > 2$.
  - Clustering of DLAs at $z \sim 2$:
    $b_{DLA}(z = 2) \simeq 2.0 \pm 0.1 \;\Rightarrow\; b_{HI} \approx 2$
  - HI intensity mapping at $z \sim 0.8$ provide an upper and a lower limit on $\Omega_{HI}\, b_{HI}(z = 0.8)$ consistent with $b_{HI}(z \simeq 1) \sim 1$.

Modeling 21 cm

Hydrodynamic simulations and semi-analytic models suggest a halo occupancy that looks like

$$M_{HI} \propto M_h^{\alpha} \ \exp\left[-\frac{M_{\rm min}}{M_h}\right]$$

- Power-law index regulated by how fast HI accretes onto halos. Simulations suggest $\alpha \approx 1$ at $z > 2$, with expectations that $\alpha < 1$ because tidal interactions, ram-pressure stripping, mergers more efficient at removing HI than cooling hot gas.
- Low mass cutoff, $M_{\rm min} \sim 10^9\, h^{-1} M_\odot$, where self-shielding becomes inefficient, constrained by clustering (where available) $\Rightarrow$ low mass halos: numerous (low shot noise) and less biased (easier to model).

Galaxy-based model

Alternatively can assume HI content of galaxies depends upon stellar mass (Dave+13). 'HI richness':

$$\frac{M_{HI}}{M_\star} \simeq 0.2 \left(\frac{M_1}{M_1 + M_\star} \right)^{0.4} \quad , \quad M_1 \approx 3 \times 10^8 M_\odot$$

roughly independent of redshift. Low mass cut-off imposed by steep fall in $M_\star$ with M_h at low M_h, evolution imposed by evolution in $M_\star - M_h$ relation.

Results qualitatively similar to the HOD model of the previous slide.

Calibration

Can adjust the model parameters to match what observations we have on abundance and clustering:

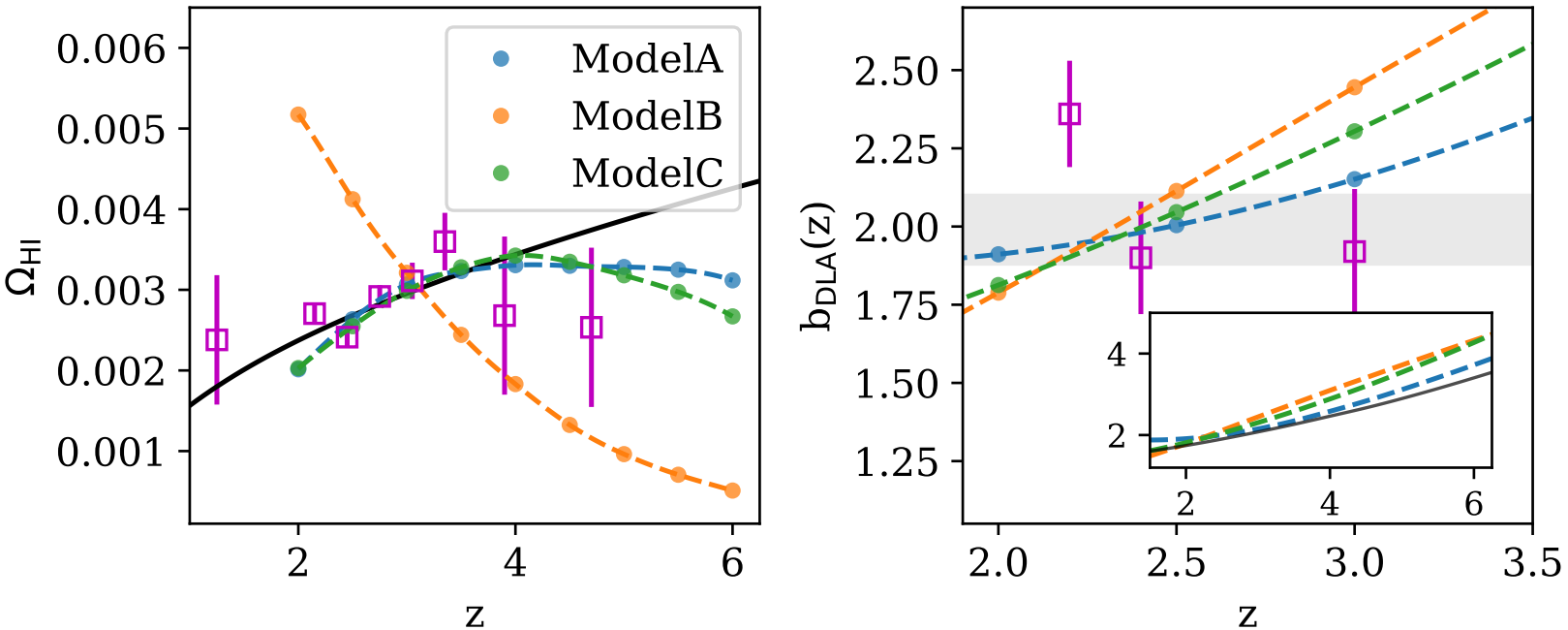

Modi+19

Intensity mapping

Review: Kovetz+ arXiv:1709.09066
Give up on resolving individual galaxies, put S/N where you want it (quasi-linear modes). Overall HI still traces δ:

	Traditional	IM
Focus	individual objects	cosmic web (quasi-linear modes)
Design	small number of capable elements	large number of passive elements
Resolution	high	low ($k_{\rm max} \sim 1\,h\,{\rm Mpc}^{-1}$)
Allocation	PI led	survey

(Galaxy people who don't resolve stars do this all the time!)

Instrument noise (FWIW)

In addition to shot-noise we have some "thermal" noise:

$$P_{21}(k,\mu) \simeq \bar{T}^2 \left(b_{HI} + f\mu^2\right)^2 P_m(k) + \bar{T}^2 P_{SN} + P_{\rm th}.$$

where

$$P_{th} = T_{\rm sys}^2 \left(\frac{\lambda^2}{A_{\rm e}}\right)^2 \left(\frac{4\pi f_{\rm sky}}{\Omega_p(z)}\right) \frac{1}{n_{\rm pol}\nu_0 t_{\rm obs} n(\vec{u})} \frac{d^2V}{d\Omega\, d(\nu/\nu_0)}$$

and

$$\frac{d^2V}{d\Omega\, d(\nu/\nu_0)} = \chi^2 \frac{d\chi}{dz} \nu_0 \frac{dz}{d\nu} = \chi^2 \frac{c\,(1+z)^2}{H(z)} \quad .$$

and

$$T_{\rm sys} = \underbrace{55\,{\rm K}}_{\rm ampl} + \underbrace{2.7\,{\rm K}}_{\rm CMB} + \underbrace{30\,{\rm K}}_{\rm grnd} + \underbrace{25\,{\rm K}\left(\frac{\nu_{\rm obs}}{400\,{\rm MHz}}\right)^{-2.75}}_{\rm sky}$$

Foregrounds

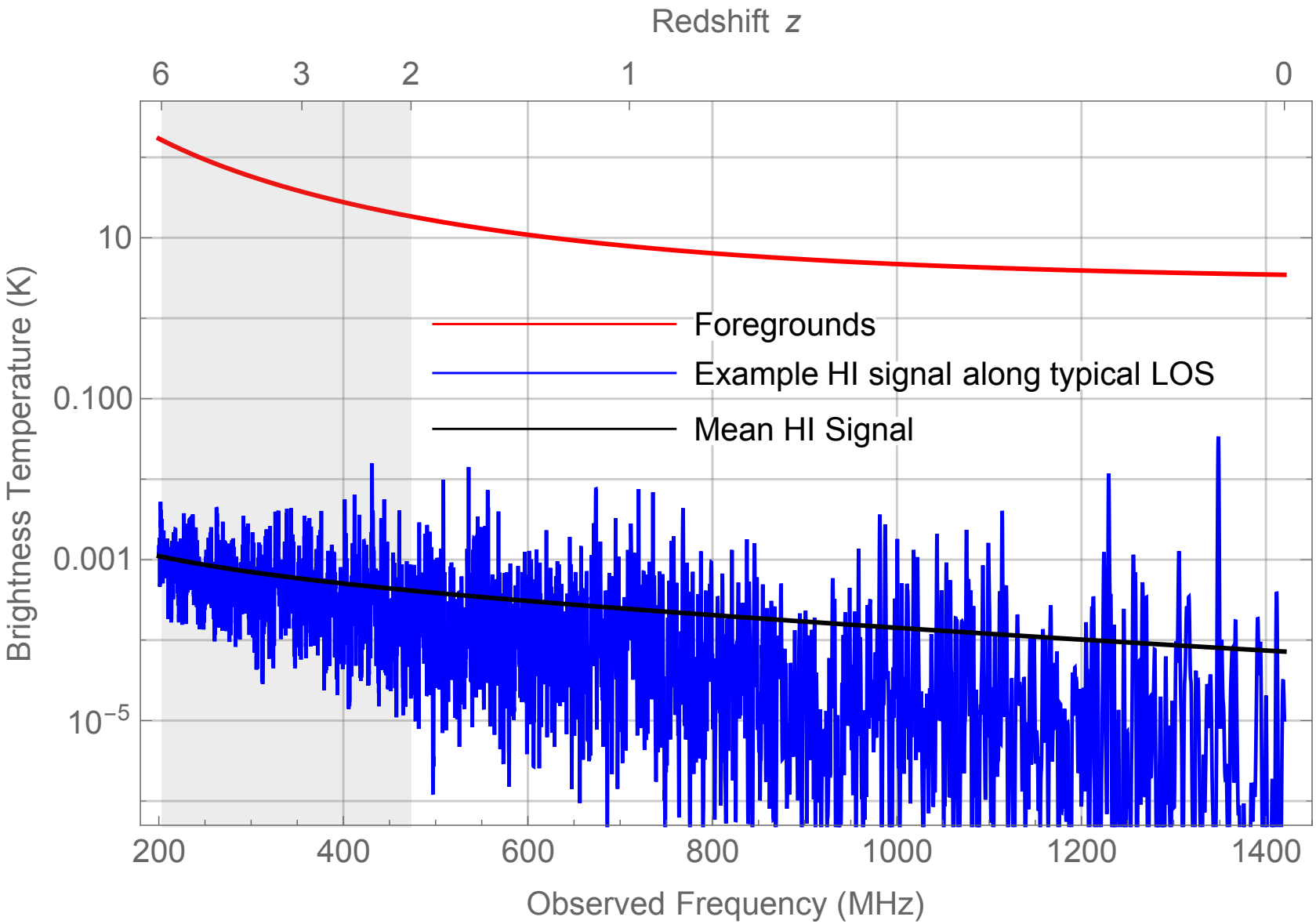

Foregrounds

- Foreground amplitude is orders of magnitude larger than the signal.
- Primarily galactic (synchrotron and free-free) and unresolved point sources.
- Spectrally smooth $\Rightarrow$ filter out low $k_{\parallel}$ modes (high-pass filter).
- A variety of methods could be used for the filter ...

Foreground wedge

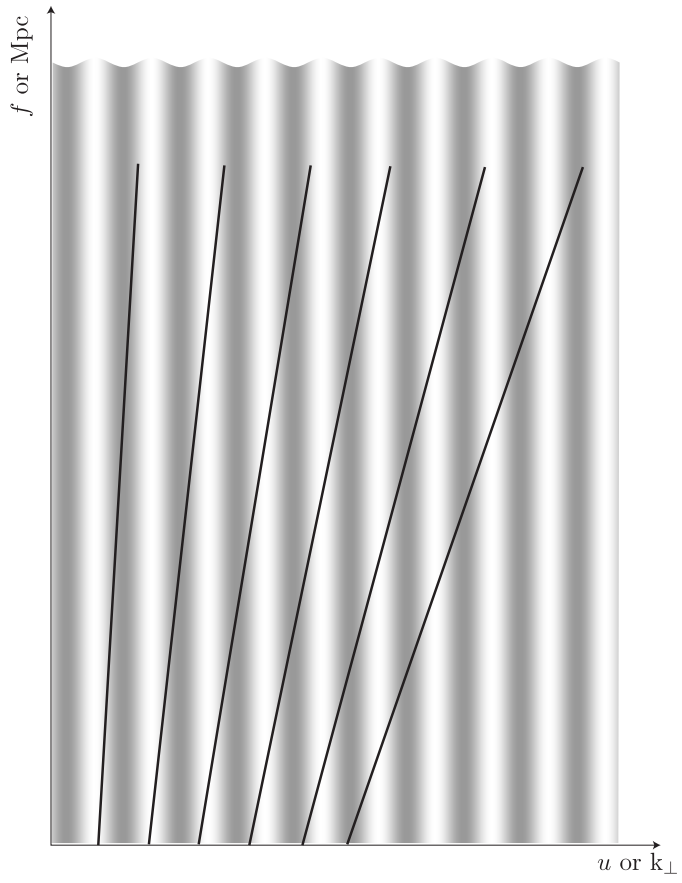

Morales+19

- Wedge arises because a baseline probes ν-dependent $k_\perp$.
- Consider a foreground with $k_\parallel \approx 0$ (grey bands).
- Baseline miscalibration adds structure along $k_\parallel$.
- Worst at high $k_\perp$, where run of $k_\perp(\nu)$ strongest.
- Leads to "foreground wedge".
- Problem more pronounced at higher z.
- Purely technical challenge!

Foreground wedge

Due to foregrounds modes with

$$\frac{k_\parallel}{k_\perp} < \sin\theta\ \mathcal{R} \quad , \quad \mathcal{R} \equiv \frac{\chi(z)\,H(z)}{c(1+z)} = \frac{E(z)}{1+z}\int_0^z \frac{dz'}{E(z')}$$

are lost.

The value of θ is under debate in the community!

$\theta = \pi/2$ is known as the "horizon wedge".
$\theta =$FOV or $\theta = 3\times$FOV are more optimistic.

Foreground wedge

$S/(S+N)$, including shot-noise and instrument noise, for a Stage II 21-cm interferometer designed for LSS studies.

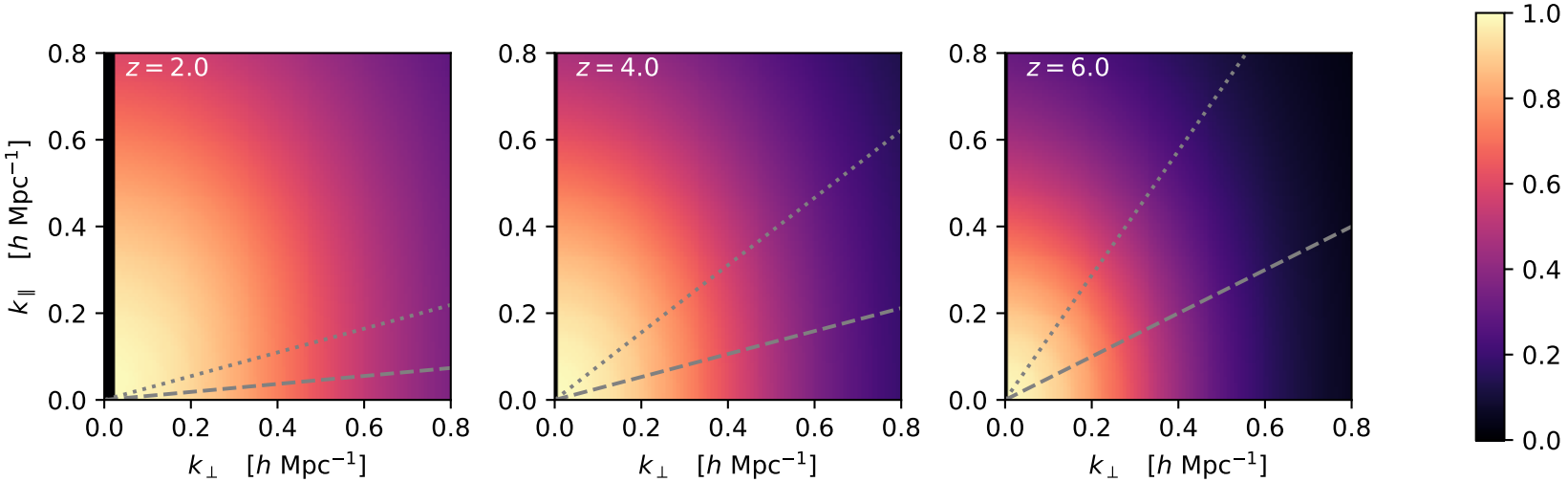

The foreground wedge for 1×FOV and 3×FOV are shown as the dashed and dotted lines (respectively).

Comparison: k-space

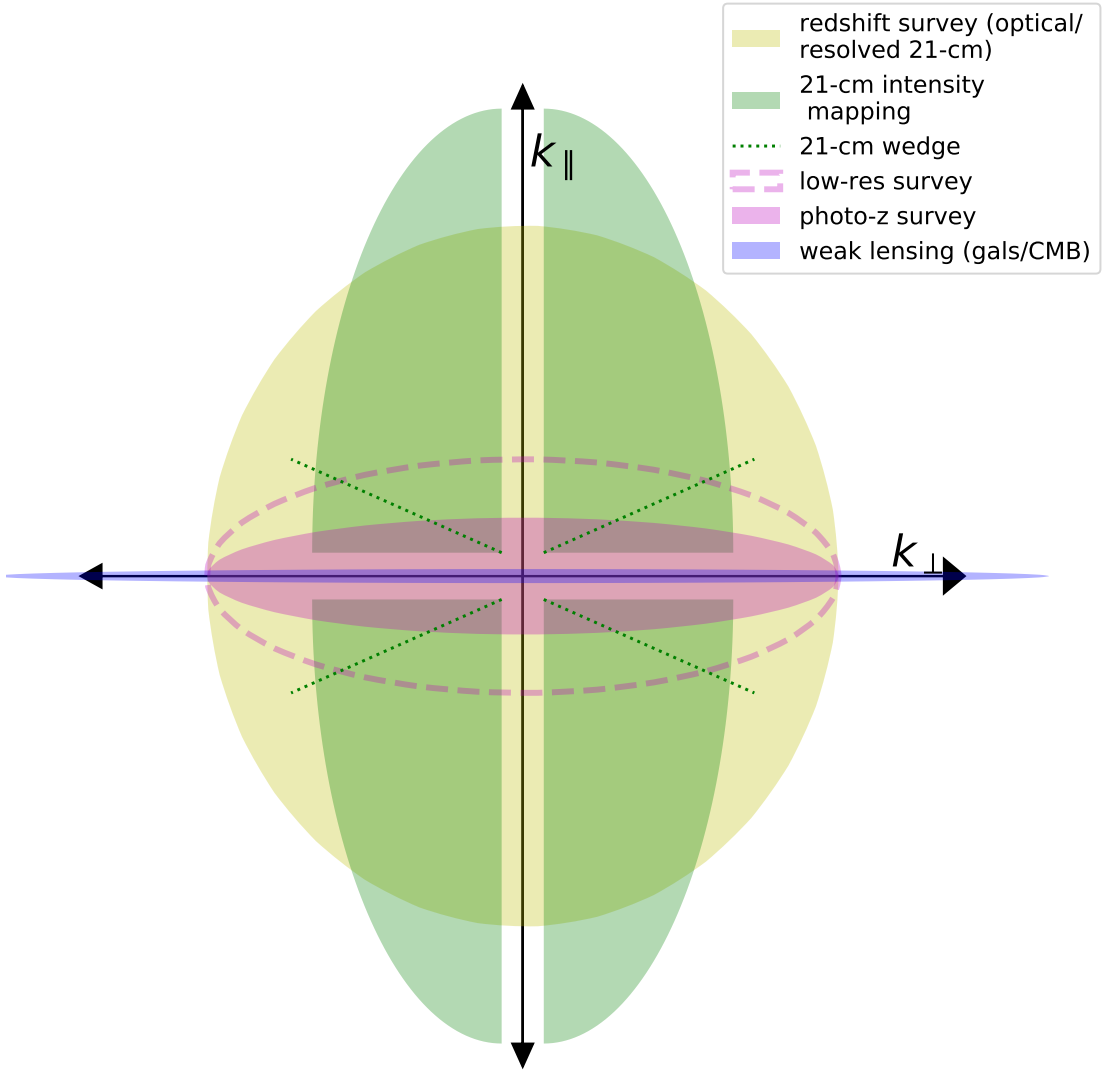

https://github.com/slosar

Experimental landscape

- HI is relatively well studied in the $z \simeq 0.1$ Universe.
- Clustering has been bounded with single-dish, GBT data at $z \simeq 1$ (see earlier).
- Currently the CHIME experiment is the "leader", but they have no cosmology results to date.
- Various other surveys in commissioning, construction or planning (some links later ...)

PUMA

The **P**acked **U**ltra-wideband **M**apping **A**rray

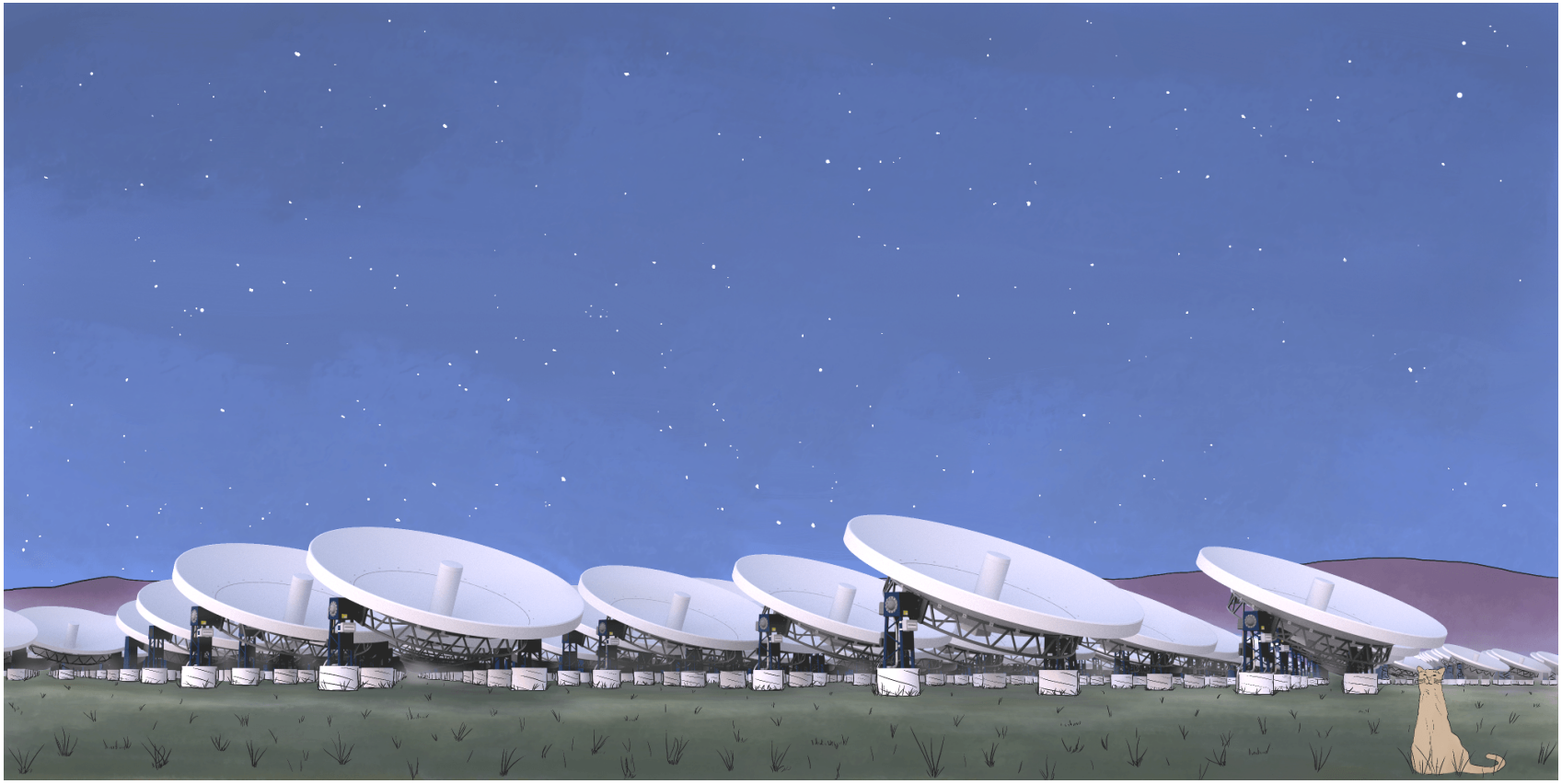

$10^3 - 10^4$, transiting 6 m dishes with $200 - 1100$ MHz receivers.

Science drivers

1. Characterize the expansion history in the pre-acceleration era.
2. Characterize structure growth in the pre-acceleration era.
3. Constrain (or detect) primordial non-Gaussianity.
4. Constrain (or detect) features in the primordial $P(k)$.
5. Fast radio burst (FRB) tomography.
6. Monitor all pulsars discovered by SKA.

arXiv:1810.09572

Science $\rightarrow$ Instrument

The science goals naturally determine the basic parameters of the experiment:

- To resolve quasi-linear modes $\Rightarrow$ longest baseline required and thus linear extent of the array ($\simeq 1.5\,\mathrm{km}$).
- Required sensitivity $\Rightarrow$ determines $N\,D > 200\,\mathrm{km}$.
- Low $k_\perp$ sensitivity $\Rightarrow$ close-packed.
- Good beam-forming sets minimum $D \simeq 6\,\mathrm{m}$.

Making mocks: HI is simple to model

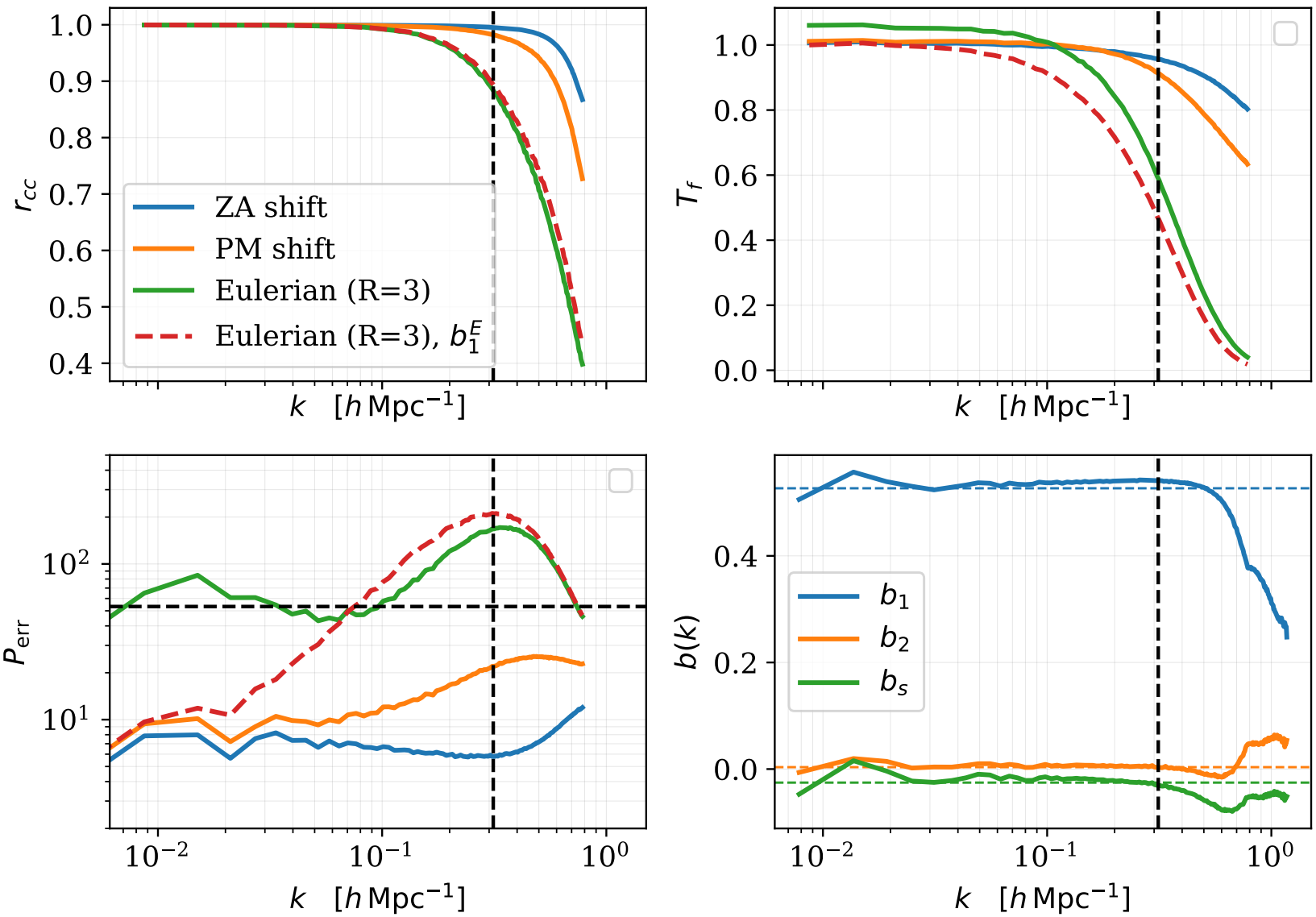

Modi+19

Fitting spectra: HI is simple to model

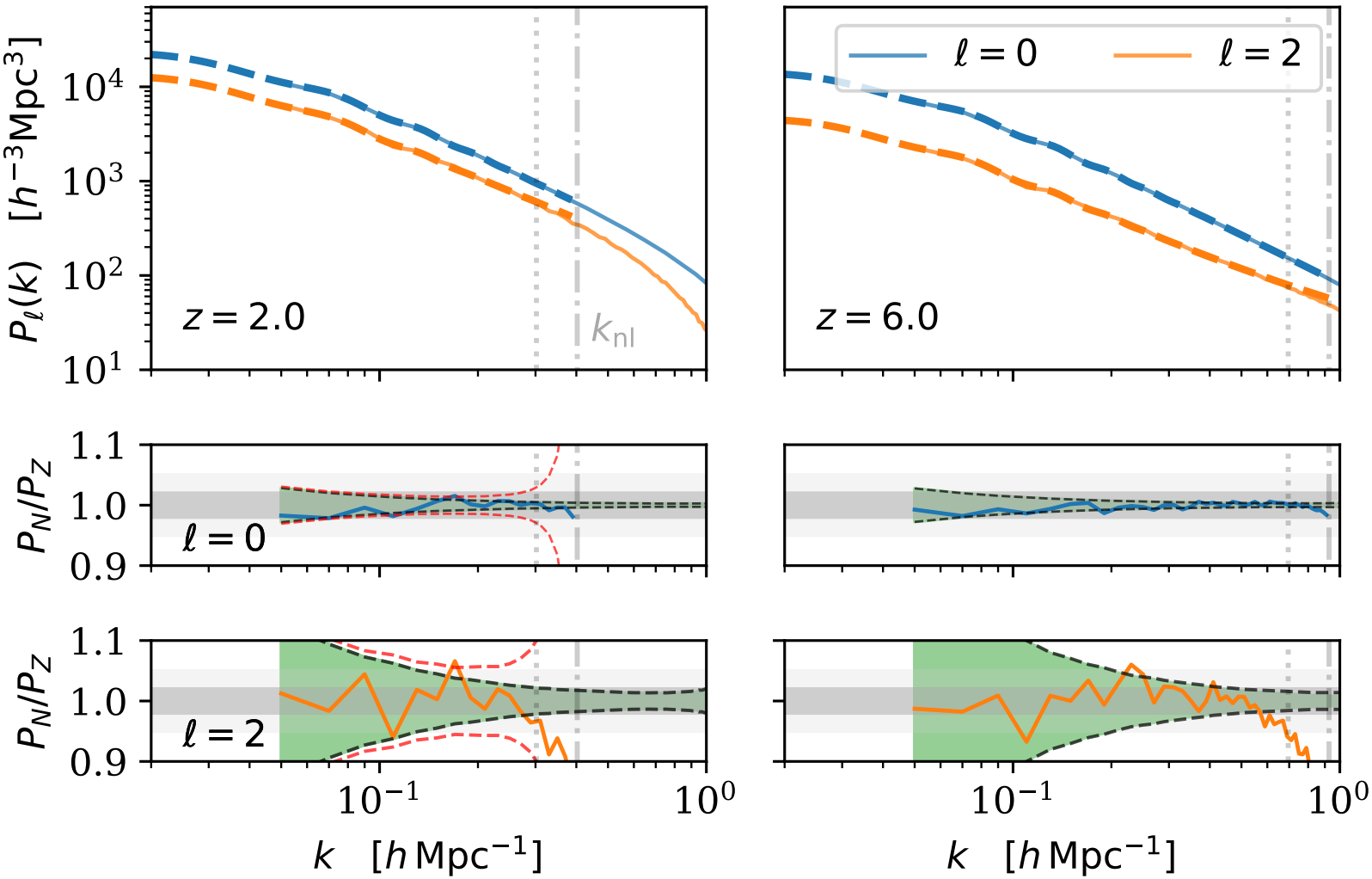

Lowest order LPT already does well ...

Modi+19

Challenges and opportunities

Numerous hardware challenges, but also

- New science cases, new approaches (missing low-$k_{\parallel}$, the wedge, uncertain $\bar{T}$).
- Calibration and analysis (foregrounds, RFI, beamforming, processing algorithms all 'at scale').
- Simulations (theory, mocks, end-to-end).
- High-performance computing ('big data': $> 10^2$ TB/day).

This field is like galaxy surveys of the 1990's or 2000's, and much of the CMB/LSS technology still needs to be rethought and adapted to this science.

Resources

- Kovetz+18
- CVDE white paper: arXiv:1810.09572
- Interferometric 21-cm, LSS experiments:
  - https://chime-experiment.ca,
  - (https://www.ska.ac.za/gallery/meerkat/)
  - OWFA
  - http://tianlai.bao.ac.cn/
  - https://hirax.ukzn.ac.za,
  - https://www.puma.bnl.gov
- Software
  - CRIME and CoLoRe
  - CORA, driftscan and draco.
  - https://github.com/andreimesinger/21cmFAST
  - https://gitlab.com/radio-fisher/bao21cm
- Mock data
  - http://cyril.astro.berkeley.edu

The End!

Dirac equation and magnetic dipole

- At low E we can ignore 2^{nd} quantization for $e^{\pm}$.
- Then $H_D = \alpha \cdot \mathbf{p} + \beta m$ with $\alpha_i^2 = \beta^2 = 1$ and $\{\alpha_i, \alpha_j\} = \{\alpha_i, \beta\} = 0$.
- In the NR limit ($E \approx mc^2$) in the standard representation with 2-spinors $\psi_\pm$ this becomes:

$$\begin{pmatrix} m - E & \sigma \cdot \mathbf{p} \\ -\sigma \cdot \mathbf{p} & m + E \end{pmatrix} \begin{pmatrix} \psi_+ \\ \psi_- \end{pmatrix} = \begin{pmatrix} 0 \\ 0 \end{pmatrix}$$

- For NR particles

$$\psi_- \approx \frac{\sigma \cdot \mathbf{p}}{2m} \psi_+ \quad \Rightarrow \quad (E - m)\psi_+ = \frac{(\sigma \cdot \mathbf{p})^2}{2m} \psi_+$$

- Including $\mathbf{B}$ field takes $\mathbf{p} \to \mathbf{p} - q\mathbf{A}$ so using σ identities

$$H_{\text{hf}} = \frac{e}{2m} \left[\mathbf{p} \cdot \mathbf{A} + \mathbf{A} \cdot \mathbf{p}\right] - \mu_B \sigma \cdot \mathbf{B}$$

with the last term $2(\mu_B/\hbar)\ \mathbf{S} \cdot \mathbf{B}$ that we need.

Hyperfine energy splitting

Recall the hyperfine levels arise from the coupling of the proton and electron spin, described by

$$H_{\rm hf}^{\ell=0} \propto \frac{e^2\, g_p\, g_e}{m_p\, m_e}\, \delta^{(3)}(\mathbf{r})\, \mathbf{S}_p \cdot \mathbf{S}_e$$

The states are defined by S^2, S_p^2 and S_e^2 and we want

$$\langle n\ell s s_p s_e \left| H_{\rm hf} \right| n\ell s s_p s_e \rangle$$

But

$$\langle \mathbf{S}_p \cdot \mathbf{S}_e \rangle = \frac{\hbar^2}{2}\left(\langle S^2 \rangle - \frac{3}{2} \right) = \frac{\hbar^2}{4} \begin{cases} +1 & s = 1 \\ -3 & s = 0 \end{cases}$$

and for the g.s. of H we have $\left\langle \delta^{(3)}(\mathbf{r}) \right\rangle = |\psi_{100}(\mathbf{0})|^2 = 1/\pi a^3$. This gives $\Delta E \simeq 6\,\mu\,\mathrm{eV}$.

Notes

- Classically $dE/dt \sim \ddot{\mu}^2 \sim \omega^4 \mu^2 \Rightarrow$ Rate$\sim \frac{\omega^4 \mu^2}{\hbar \omega} \sim \omega^3 \mu^2$.
- In QM Fermi Golden rule says

$$R \sim \frac{2\pi}{\hbar} \delta(\Delta E - \hbar\omega) \left| \langle f | V | i \rangle \right|^2$$

- Have $V \sim \vec{A}$, with $A \ni \omega^{-1/2} \epsilon_{k\lambda} a^\dagger_{k\lambda} \exp[ikx]$ (normalized so that $H \sim E^2 + B^2 \sim (\partial A)^2 \sim \hbar\omega a^\dagger a$).
- Final state $d^3k \sim k^2\, dk\, d\Omega$. Use the δ-fn to kill dk, the $\omega^{-1/2}$ squared kills one k.
- Summing over λ gives $P_{ij} = \delta_{ij} - \hat{k}_i \hat{k}_j$
- Magnetic dipole comes from ikx from exponential.

Hyperfine transition rate

- The transition rate can be computed from Fermi's Golden Rule with an interaction $\propto \mathbf{S}_e$ (and 2^{nd} quantized radiation).
- The $\vec{E}$-dipole transition is zero by parity.
- The transition proceeds via the magnetic dipole for the e^-, e.g.

$$R_{\downarrow\uparrow} \propto \omega^3 \, \mathcal{P}_{ij} \left\langle \downarrow \left| \mathbf{S}_i^e \right| \uparrow \right\rangle^\dagger \left\langle \downarrow \left| \mathbf{S}_j^e \right| \uparrow \right\rangle$$

  (i.e. it is a *forbidden* transition).
- Find

$$\begin{aligned} A_{10} &= \frac{64\,\pi^4\,\mu_B^2}{3\,h\,\lambda^3} \qquad (\propto \omega^3 \mu_B^2) \\ &\simeq 2.85 \times 10^{-15}\,\mathrm{s}^{-1} \end{aligned}$$

The cosmic web

- A natural outcome of gravitational instability from Gaussian ICs is a beaded filamentary network of voids, sheets, filaments and knots known as the cosmic web.
- All of galaxy and structure formation occurs in this context!

Protoclusters and voids at $z = 1$

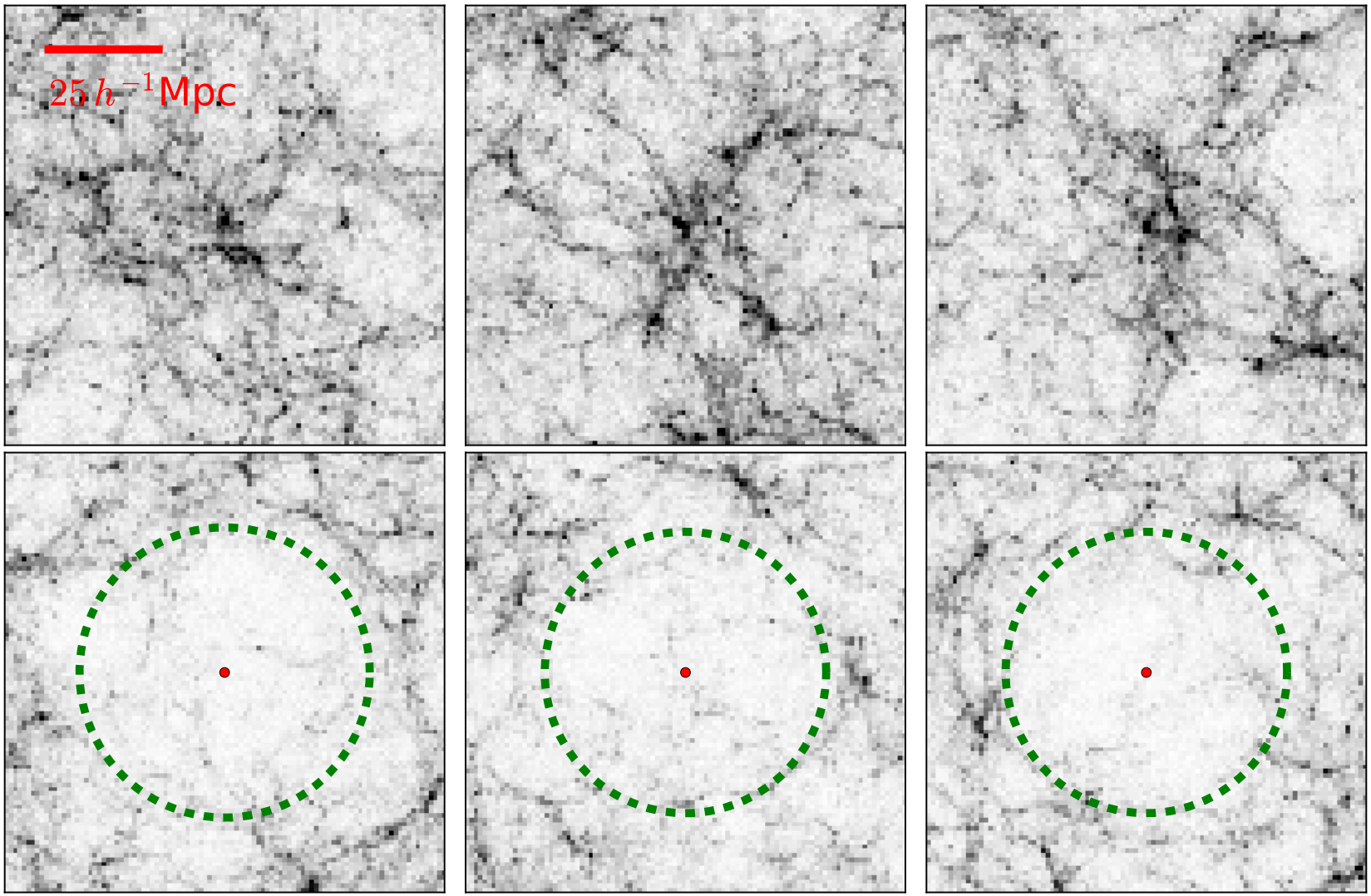

Protoclusters and voids at $z = 1$

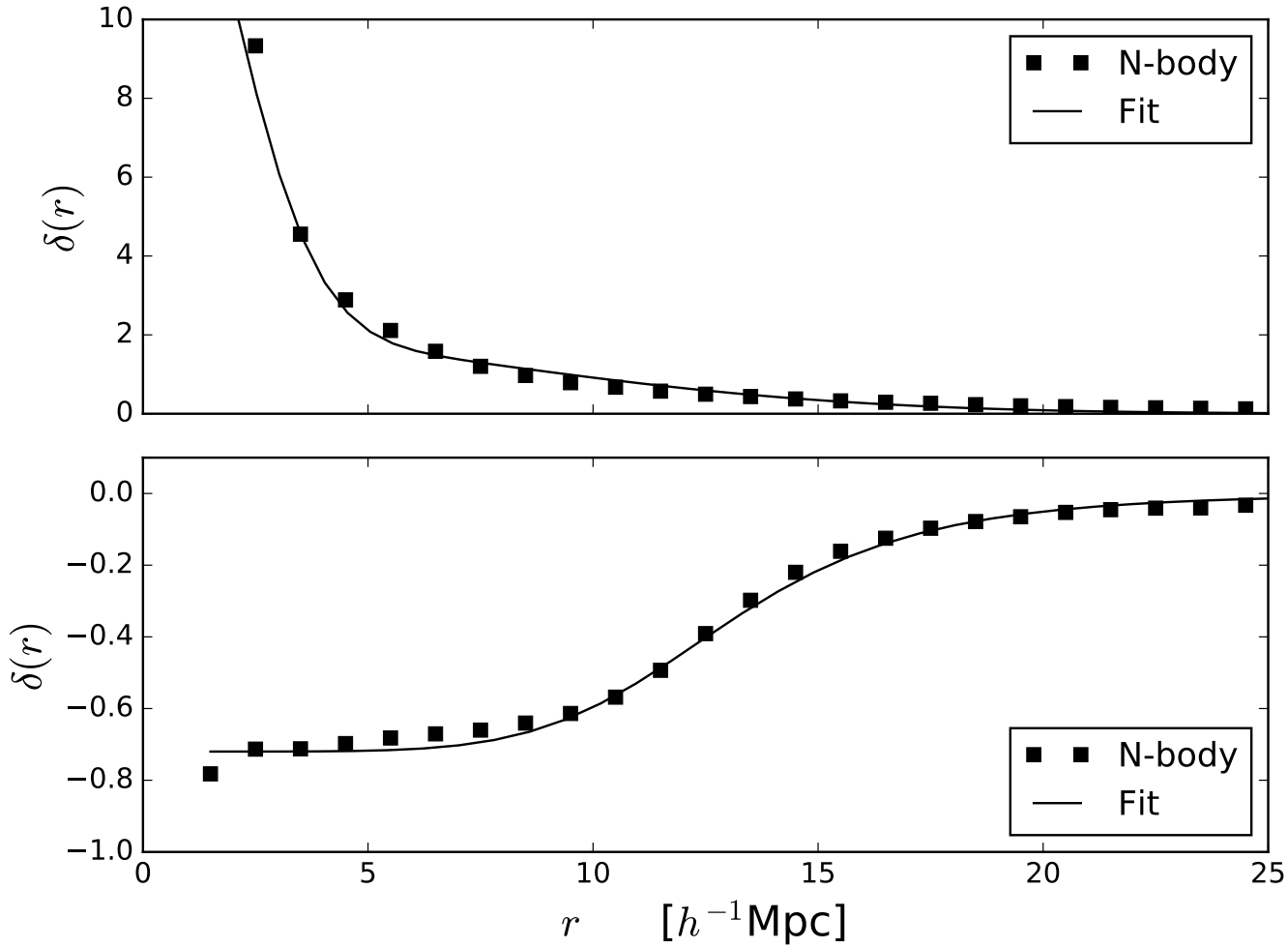

Protoclusters and voids in the dark matter extend coherently over $\mathcal{O}(10\,\mathrm{Mpc})$.

Matched filter

- Suppose I have some data, $\vec{d}$, buried in which is a signal, $\vec{s}$, which I would like to find.
- A classic method is the "matched filter".
- Assume $\vec{d} = A\,\vec{s} + \vec{n}$, with $\vec{n}$ Gaussian noise.
- Then $\vec{d} - A\,\vec{s}$ is Gaussian

$$-2\ln\mathcal{L} = \left(\vec{d} - A\,\vec{s}\right)^T N^{-1} \left(\vec{d} - A\,\vec{s}\right) + \text{const}$$

- This is a Gaussian in A with

$$\langle A \rangle = \frac{\vec{s}^T N^{-1} \vec{d}}{\vec{s}^T N^{-1} \vec{s}} \qquad , \qquad \sigma_A^{-2} = \underbrace{\vec{s}^T N^{-1} \vec{s}}_{\text{Fisher scalar}}$$

- Note: simply a vector dotted into $\vec{d}$.
- Vary the parameters of $\vec{s}$ (e.g. location and size) to maximize signal-to-noise ratio.

Protoclusters and voids at $z = 1$

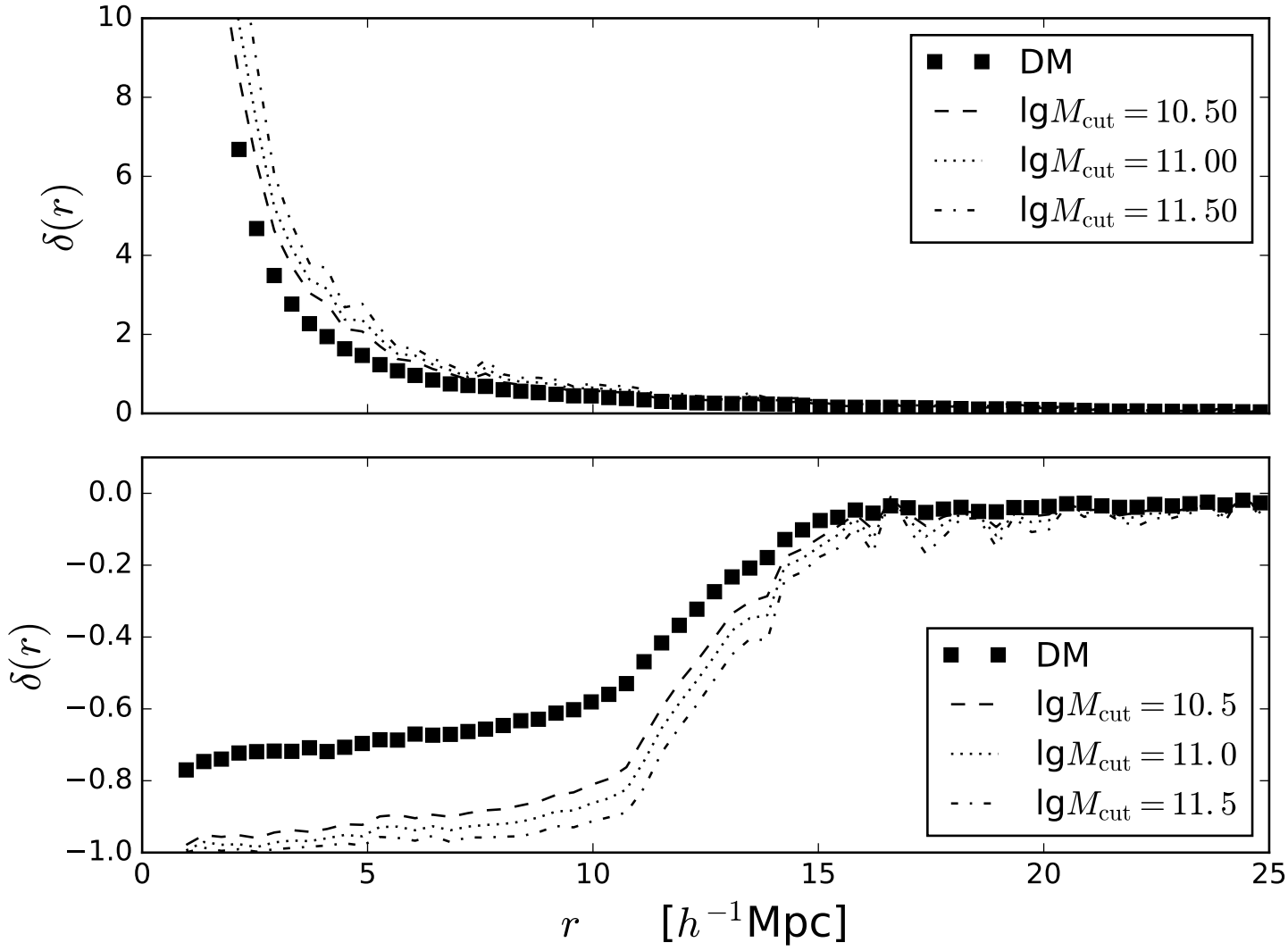

Such HODs predict signal of protoclusters and voids at least as strong as in the matter.

Beam

For a parabola the distance to the focus and directrix are equal.

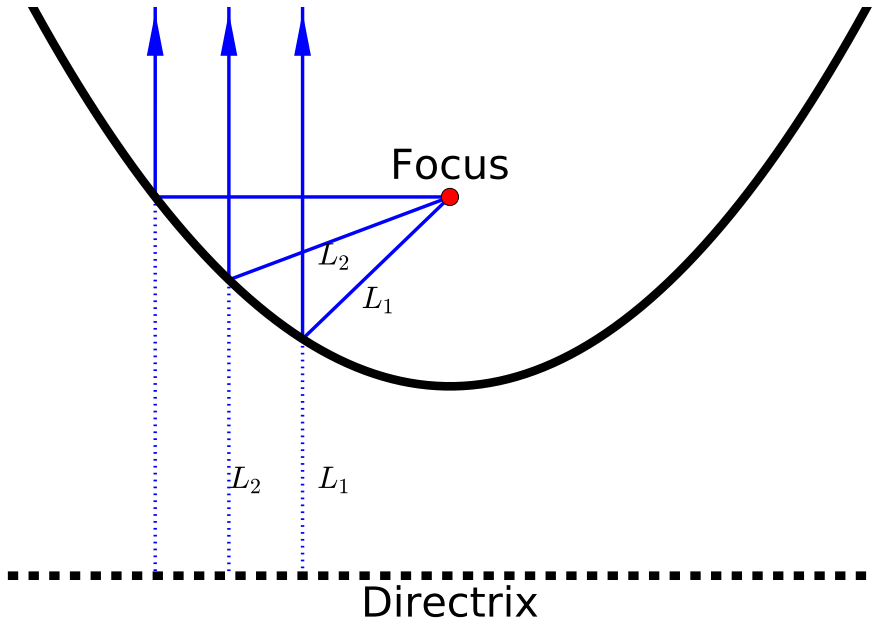

Illuminating a parabola with a dipole antenna is the same as illuminating the directrix with a plane-wave like:

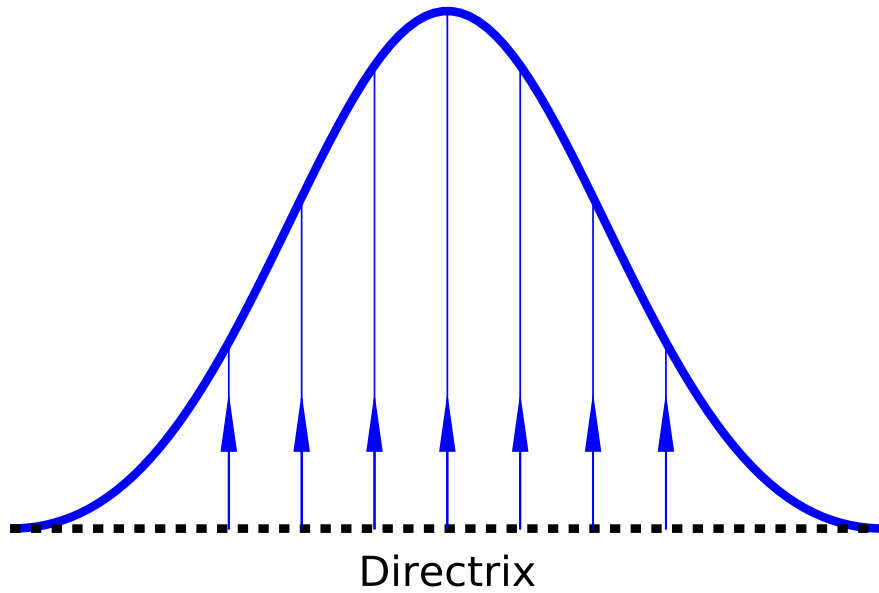

Of course, the radiation really comes in, and upon reflection all waves get a phase shift, but ...

The *m*-mode formalism and transiting telescopes

To begin, consider a single frequency, corresponding to a fixed redshift or (redshift-space) distance. Suppose our template, τ, is centered at $\theta = 0$, is ϕ-independent and non-zero only when $\theta \ll 1$. We expand

$$\begin{aligned}
\tau_{\ell m} &= \int d\hat{n}\; Y^{\star}_{\ell m}(\hat{n})\,\tau(\theta) \\
&= 2\pi\,\delta_{m0}\sqrt{\frac{2\ell+1}{4\pi}}\int d(\cos\theta) P_{\ell}(\cos\theta)\,\tau(\theta) \\
&\simeq \delta_{m0}\sqrt{\frac{2\ell+1}{4\pi}}\;\left[2\pi\int \tilde{\omega}\,d\tilde{\omega}\; J_0(\ell\tilde{\omega})\,\tau(\tilde{\omega})\right]
\end{aligned}$$

where in the last line we have defined $\tilde{\omega} = 2\sin(\theta/2) \simeq \theta$ and used $P_{\ell}(\cos\theta) \approx J_0(\ell\theta)$ for $\theta \ll 1$.

The *m*-mode formalism and transiting telescopes

- The $\sqrt{(2\ell+1)/4\pi}$ is just $Y_{\ell 0}(\hat{z})$.
- If we extend the upper limit of $\tilde{\omega}$-integration to infinity, we recognize in the brackets on the last line

$$\left[2\pi \int \tilde{\omega}\, d\tilde{\omega}\; J_0(\ell\tilde{\omega})\, \tau(\tilde{\omega})\right]$$

  the Hankel transform of τ.
- i.e. the 2D Fourier transform of τ with spherical symmetry.

$$\tau_{\ell m} \simeq \delta_{m0} \underbrace{\sqrt{\frac{2\ell+1}{4\pi}}}_{Y_{\ell 0}(0,0)} \underbrace{\left[2\pi \int \tilde{\omega}\, d\tilde{\omega}\; J_0(\ell\tilde{\omega})\, \tau(\tilde{\omega})\right]}_{\text{FT of } \tau}$$

The *m*-mode formalism and transiting cylinders

- Now we can rotate the template from the north pole to an arbitrary $\hat{n}$ using Wigner functions, $\mathcal{D}^{\ell}_{m'm}$.
- However, in our case $\tau_{\ell m} \propto \delta_{m0}$ and

$$Y_{\ell m} = \sqrt{\frac{2\ell+1}{4\pi}}\, \mathcal{D}^{\ell}_{0m} \tag{1}$$

- The spherical harmonic coefficients for a template centered on $\hat{n}$ are

$$\begin{aligned} \tau_{\ell m}(\hat{n}) &= \sqrt{\frac{4\pi}{2\ell+1}}\, Y^{\star}_{\ell m}(\hat{n})\, \tau_{\ell 0}(\hat{z}) & (2)\\ &= \left[2\pi \int \tilde{\omega}\, d\tilde{\omega}\; J_0(\ell\tilde{\omega})\, \tau(\tilde{\omega})\right]\, Y^{\star}_{\ell m}(\hat{n}) & (3) \end{aligned}$$

(with no implied sum over ℓ).

The m-mode formalism and transiting cylinders

- These $\tau_{\ell m}$ can now be inserted into our formula for the m-mode visibility to obtain

$$V_{ij}^{m} = \sum_{\ell} B_{ij}^{\ell m}\, Y_{\ell m}^{\star}(\hat{n}) \left[2\pi \int \tilde{\omega}\, d\tilde{\omega}\; J_0(\ell\tilde{\omega})\, \tau(\tilde{\omega}) \right] \qquad (4)$$

- This is the central relation needed for the matched filter, as it expresses a linear relationship between the observable and the template.
- We recognize the the combination $B_{ij}^{\ell m}\, Y_{\ell m}^{\star}$ as the beam transfer function, $B_{ij}(\hat{n};\phi)$, evaluated at the position of the object but now modulated by the Fourier transform of τ.

The *m*-mode formalism and transiting cylinders

- If we now perform the Fourier transform in frequency, the term in square brackets becomes the 3D Fourier transform for an azimuthally symmeteric function in cylindrical coordinates: $\tau(k_\perp, k_\parallel)$ with $\ell \simeq |k_\perp|$.
- For a narrow range of frequencies (corresponding to an astrophysical object such as a void or protocluster for example) the $k_\perp$ probed by the interferometer are almost constant.
- The generalization to non-symmetric profiles is straightforward, but not very enlightening.